

# Anthraceno-Cryptands: A New Class of Cation-Complexing Macrobicyclic Fluorophores

Frédéric Fages,<sup>†</sup> Jean-Pierre Desvergne,<sup>\*†</sup> Henri Bouas-Laurent,<sup>\*†</sup> Pierre Marsau,<sup>†</sup> Jean-Marie Lehn,<sup>\*§</sup> Florence Kotzyba-Hibert,<sup>§</sup> Anne-Marie Albrecht-Gary,<sup>\*||</sup> and Malak Al-Joubbeh<sup>||</sup>

Contribution from the Laboratoire de Photochimie Organique, CNRS U.A. 348, 351 Cours de la Libération, 33405 Talence Cedex, France, Cristallographie et Physique Cristalline, CNRS U.A. 144, 351 Cours de la Libération, 33405 Talence Cedex, France, Chimie Organique Physique, CNRS U.A. 422, Institut Le Bel, 4 Rue Blaise Pascal, 67000 Strasbourg, France, and Chimie Physique et Electroanalyse, CNRS U.A. 405, EHICS, 67000 Strasbourg, France.  
Received April 24, 1989

**Abstract:** A new class of macrobicyclic and cation photosensitive compounds, the anthraceno-cryptands  $A_{nn}$  is described. In these ligands, the nitrogen lone pairs form intramolecular exciplexes with the anthracene ring, inducing a dual fluorescence emission (monomer type and exciplex) sensitive to the nature of the solvent. Thus, although  $A_{22}$  displays an intense triple exciplex emission in aprotic solvents, only a strong monomer-type emission is observed in methanol; this behavior is ascribed to hydrogen bonds between the solvent and the nitrogen lone pairs, which maintain an out-out conformation preventing exciplex formation. For  $A_{33}$ , the two nitrogens do not appear to be simultaneously involved in the solvation as a dual emission is recorded in methanol. Anthraceno-cryptands  $A_{nn}$  present drastic changes in fluorescence emission upon complexation by alkali-metal cations and protons; the fluorescence spectrum displays a hypsochromic shift and the quantum yield is enhanced. Comparison with the reference molecules, i.e., the macrocyclic "crowned" molecules ( $M_n$ ) and 9,10-di-*n*-propylanthracene ( $R$ ), shows that the spectroscopic response is related (i) to the ability of the cation to suppress the nitrogen-anthracene interaction (ii) to the distance separating the aromatic  $\pi$  cloud and the cation. Unusual interactions between heavy-metal cations ( $Tl^+$  and  $Ag^+$ ) and anthracene have been revealed: a novel complex with  $Tl^+$  and an exciplex with  $Ag^+$  have been described. The stoichiometry and the stability constants of the complexes with protons and metal cations ( $Tl^+$  and  $Ag^+$ ) have been determined by spectrometric titrations.

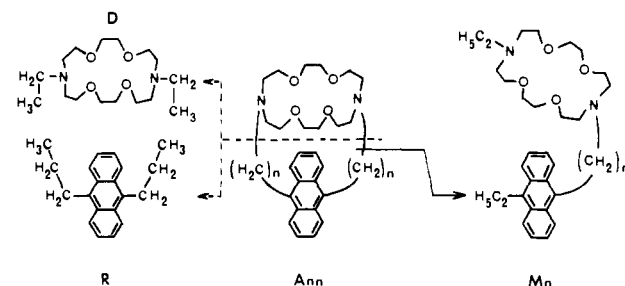
A number of new compounds whose electronic absorption and emission spectra and photochemical reactivity are markedly affected by the presence of cations or, conversely, whose complexing ability can be significantly changed by photochemical reactions have been synthesized and investigated during the last decade.<sup>1a-c</sup> This may lead to the conception of light-driven ionic molecular devices<sup>2</sup> that release or take up ionic species under irradiation; one may thus envisage the generation of reversible photoinduced ion pulses.

The fluorescence of aromatic hydrocarbons is most often quenched by inorganic salts,<sup>3</sup> but moderate fluorescence enhancements have been observed with the macrocyclic polyethers dibenzo-18-crown-6 and 1,8-naphtho-21-crown-6 in the presence of alkali-metal cations.<sup>1c,e,f</sup> Aromatic chromophores incorporated into ligands stronger than monocyclic ethers, such as cryptands, were expected to exhibit more pronounced photophysical responses in the presence of salt,<sup>1g</sup> and some of us reported a preliminary study<sup>4</sup> of two anthraceno-cryptands  $A_{nn}$  ( $n = 2, 3$ ) (Scheme I) that combine the complexing ability of the cryptands<sup>5</sup> and the photophysical properties of the anthracene ring,<sup>6</sup> in particular an intense fluorescence emission; the latter can be quenched by formation of intramolecular exciplexes<sup>7</sup> between the aromatic ring and the nitrogen lone pairs and restored by protonation or metal cation complexation by the [18]- $N_2O_4$  macrocyclic moiety of compounds  $A_{nn}$ . In parallel, anthracenoyl cryptands were used as fluorescence probes for membrane studies.<sup>8</sup>

Along these lines, strong fluorescence enhancements were observed with 9-anthrylmethyl-substituted monoazacrown ethers<sup>1j</sup> and with 9,10-(TMEDA)<sub>2</sub>-substituted anthracenes.<sup>10</sup> Important modifications of fluorescence emission with heterocycles linked to azacrown ethers have been noted.<sup>1m,n</sup>

Another advantage of the anthraceno-cryptands is that they appear well suited to examination of the interaction of the nitrogen lone pairs with the aromatic ring in a given arrangement. Moreover, they were also designed to bring new insights into

**Scheme I.** Anthraceno-cryptands  $A_{nn}$  ( $n = 2, 3$ ) and Their Monochromophoric  $R$  and Trichromophoric  $M_n$  Reference Compounds<sup>a</sup>



<sup>a</sup>The 1,10-diaza crown ether D is the complement to R.

oriented proximity interactions between metal cations and  $\pi$  systems. Similar molecules appeared recently,<sup>2</sup> which can be used

- (1) (a) Löhr, H.-G.; Vögtle, F. *Acc. Chem. Res.* **1985**, *18*, 65. (b) Ogawa, S.; Narushina, R.; Arai, Y. *J. Am. Chem. Soc.* **1984**, *106*, 5760. (c) Larson, J. M.; Sousa, L. R. *Ibid.* **1978**, *100*, 1943. (d) Ghosh, S.; Petrin, M.; Maki, A. H.; Sousa, L. R. *J. Chem. Phys.* **1987**, *87*, 4315. (e) Shizuka, H.; Takada, K.; Morita, T. *J. Phys. Chem.* **1980**, *84*, 994. (f) Wolfbeiß, O. S.; Offenbacher, H. *Monatsh. Chem.* **1984**, *115*, 647. (g) Tundo, P.; Fendler, J. H. *J. Am. Chem. Soc.* **1980**, *102*, 1760. (h) Nishida, H.; Katayama, Y.; Katsudi, H.; Nakamura, H.; Takagi, M.; Ueno, K. *Chem. Lett.* **1982**, 1853. (i) Shinkai, S.; Ishikawa, Y.; Shinkai, H.; Tsuno, T.; Makishima, H.; Ueda, K.; Manabe, O. *J. Am. Chem. Soc.* **1984**, *106*, 1801. (j) De Silva, A. P.; De Silva, S. A. *J. Chem. Soc., Chem. Commun.* **1986**, 1709. (k) Street, K. W., Jr.; Krause, S. A. *Anal. Lett.* **1986**, *19*, 735. (l) Bouas-Laurent, H.; Castellan, A.; Daney, M.; Desvergne, J.-P.; Guinand, G.; Marsau, P.; Riffaud, M.-H. *J. Am. Chem. Soc.* **1986**, *108*, 315, and references therein. (m) Fery-Forgues, S.; Le Bris, M. T.; Guetté, J. P.; Valeur, B. *J. Chem. Soc., Chem. Commun.* **1988**, 384. (n) Fery-Forgues, S.; Le Bris, M. T.; Guetté, J. P.; Valeur, B. *J. Phys. Chem.* **1988**, *92*, 6233. (o) Huston, M. E.; Haider, K. W.; Czarnik, A. W. *J. Am. Chem. Soc.* **1988**, *110*, 4460. (p) Adams, S. R.; Kao, J. P. Y.; Grynkiewicz, G.; Minta, A.; Tsien, R. Y. *J. Am. Chem. Soc.* **1988**, *110*, 3212. (q) Stinson, S. *Chem. Eng. News* **1987**, *65*, (Nov 9), 26.

(2) Lehn, J.-M. *Angew. Chem., Int. Ed. Engl.* **1988**, *27*, 89.

(3) (a) McCullough, J. J.; Yeroushalmi, S. *J. Chem. Soc., Chem. Commun.* **1983**, 254. (b) Kitamura, N.; Imabagashi, S.; Tazuke, S. *Chem. Lett.* **1983**, 455. (c) Watkins, A. R. *J. Phys. Chem.* **1978**, *78*, 2555.

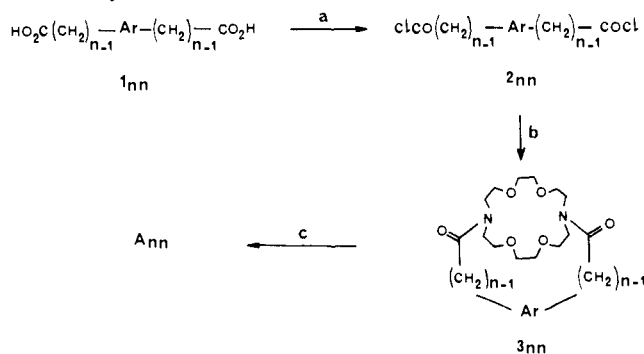
<sup>†</sup>Photochimie Organique.

<sup>‡</sup>Cristallographie et Physique Cristalline.

<sup>§</sup>Chimie Organique Physique.

<sup>||</sup>Chimie Physique et Electroanalyse.

**Scheme II.** Synthesis of Anthraceno-cryptands  $A_{nn}$  ( $n = 2, 3$ ; Ar  $\equiv$  9,10-anthrylidene)<sup>a</sup>



<sup>a</sup>(a)  $\text{SOCl}_2$ ; (b)  $[\text{18}]\text{-N}_2\text{O}_4$  macrocycle,  $\text{Et}_3\text{N}$ , benzene; (c) (i)  $\text{B}_2\text{H}_6/\text{THF}$ , (ii) 6 N,  $\text{HCl}$ , (iii)  $\text{Et}_4\text{N}^+\text{OH}^-$ .

as light conversion systems (in the presence of lanthanoid cations) or as light-to-electron conversion devices (in a zinc porphyrin macrocyclic skeleton).

We report here the results obtained on compounds  $A_{nn}$  since the preliminary communication;<sup>4</sup> some related work has been published separately.<sup>7,9</sup> We describe the synthesis, the structure determination, and the complexing ability of the ligands and the photophysical study in the absence and the presence of protons as well as of light- and heavy-metal cations. To characterize the rigid bicyclic skeleton effect of  $A_{nn}$ , several flexible reference compounds were also synthesized and studied: 9,10-di-*n*-propylanthracene (R), a monochromophoric model, 9,10-disubstituted anthracenes with a pendant  $[\text{18}]\text{-N}_2\text{O}_4$  unit ( $M_n$ ), and the  $N,N'$ -diethyl- $[\text{18}]\text{-N}_2\text{O}_4$  macrocycle (D) (Scheme I).

## Results

**Syntheses. (1) Cryptands  $A_{nn}$ .** The generalized synthetic strategy for compounds  $A_{nn}$  is outlined in Scheme II. It follows a route that allows introduction of the two different bridges  $n = 2, n = 3$  between the  $[\text{18}]\text{-N}_2\text{O}_4$  unit and the anthracene ring.

The anthracenedicarboxylic acids  $1_{nn}$  were prepared according to published procedures<sup>10</sup> and subsequently transformed into the corresponding dichlorides  $2_{nn}$  with thionyl chloride<sup>11</sup> (75% yield). High dilution condensation of  $2_{nn}$  with the  $[\text{18}]\text{-N}_2\text{O}_4$  macrocycle<sup>12</sup> affords the macrocyclic diamides respectively  $3_{22}$  (mp  $>260$  °C; 61% yield) and  $3_{33}$  (mp  $>260$  °C; 65% yield). By reduction with diborane, the diamides give the anthraceno-cryptands as yellow solid materials  $A_{22}$  (mp  $>260$  °C; 65% yield) and  $A_{33}$  (mp 215 °C; 77% yield).

**(2) Reference Compounds.** The preparation of 9,10-di-*n*-propylanthracene (R) is described in the literature.<sup>13</sup>

The synthesis of the new compounds  $M_n$  ( $n = 2, 3$ ) is outlined in Scheme III.

(4) Konopelski, J. P.; Kotzyba-Hibert, F.; Lehn, J.-M.; Desvergne, J.-P.; Fages, F.; Castellán, A.; Bouas-Laurent, H. *J. Chem. Soc., Chem. Commun.* **1985**, 433.

(5) Lehn, J.-M. *Acc. Chem. Res.* **1978**, *11*, 49.

(6) Bouas-Laurent, H.; Castellán, A.; Desvergne, J.-P. *Pure Appl. Chem.* **1980**, *52*, 2633.

(7) Fages, F.; Desvergne, J.-P.; Bouas-Laurent, H. *J. Am. Chem. Soc.* **1989**, *111*, 96.

(8) Hermann, U.; Tümmeler, B.; Maass, G.; Mew, P. K. T.; Vögtle, F. *Biochemistry* **1984**, *23*, 4059.

(9) (a) Fages, F.; Desvergne, J.-P.; Bouas-Laurent, H.; Hirschberger, J.; Marsau, P.; Pétraud, M. *New J. Chem.* **1988**, *12*, 95. (b) Guinand, G.; Marsau, P.; Lehn, J.-M.; Kotzyba-Hibert, F.; Konopelski, J. P.; Desvergne, J.-P.; Fages, F.; Castellán, A.; Bouas-Laurent, H. *Acta Crystallogr.* **1986**, *C42*, 715. (c) Marsau, P.; Bouas-Laurent, H.; Desvergne, J.-P.; Fages, F.; Lamotte, M.; Hirschberger, J. *Mol. Cryst. Liq. Cryst.* **1988**, *156*, 383.

(10) Miller, M. W.; Amidon, R. W.; Tawney, P. O. *J. Am. Chem. Soc.* **1955**, *77*, 2845.

(11) Rio, G. *Ann. Chim. (Paris)* **1954**, *9*, 182.

(12) Dietrich, B.; Lehn, J.-M.; Sauvage, J.-P.; Blanzat, J. *Tetrahedron* **1973**, *29*, 1629.

(13) Cherkasov, A. S.; Bazilevskaya, N. S. *Izv. Akad. Nauk. SSSR, Ser. Fiz.* **1965**, *29*, 1284.

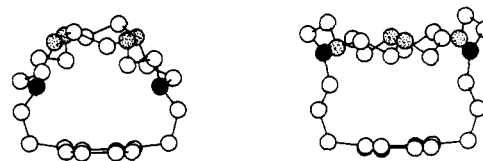


**Figure 1.** Crystal structures of the anthraceno-cryptands  $A_{22}$  (left) and  $A_{33}$  (right).

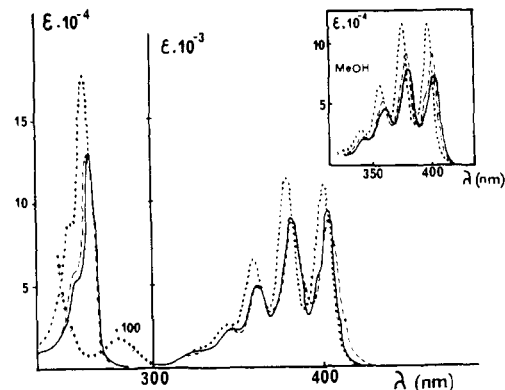


**Figure 2.** Electronic absorption spectra of  $A_{nn}$ , R, and of the  $N,N'$ -diethyl-diaza-18-crown-6 in methylcyclohexane (concentration,  $<10^{-4}$ ) at room temperature. The latter has  $\epsilon = 210 \text{ M}^{-1} \text{ cm}^{-1}$  at 285 nm.  $A_{22}$ , —;  $A_{33}$ , ---; R, ···; D, - · - ·. Inset: spectra of  $A_{22}$ ,  $A_{33}$ , and R in  $\text{CH}_3\text{OH}$ .

**Table I.** Electronic Absorption Spectral Data [ $\lambda$  (nm) Wavelength of the Maximum of the Lowest Energy Vibronic Band of the  ${}^1L_a$  Electronic Transition] for Compounds  $A_{nn}$ ,  $M_n$ , and R in Toluene and Methanol at Room Temperature<sup>a</sup>

	$\lambda$ , nm ( $\epsilon$ , $\text{M}^{-1} \text{ cm}^{-1}$ )	
	toluene	methanol
$A_{22}$	406 (9200)	402 (7800)
$A_{33}$	406 (8300)	400 (9300)
$M_2$	402 (9200)	398 (9500)
$M_3$	402 (9300)	398 (9700)
R	402 (11300)	398 (11500)

<sup>a</sup> The intensity ( $\epsilon$ ,  $\text{M}^{-1} \text{ cm}^{-1}$ ) is given in parentheses.

The ester  $7_2$  (mp 88–89 °C), obtained (80% yield) from 10-ethylanthrone<sup>14</sup> (**4**) by the Reformatsky reaction, was readily transformed into the acid  $8_2$  (mp 258 °C; 84% yield). In a similar way,  $8_3$  was obtained (mp 146 °C; 93% yield) from the ester  $7_3$  (mp 74–75 °C) prepared (79% yield) by catalytic hydrogenation of ester **6** (mp 110–111 °C). The latter was obtained (77% yield) by treating compound **5** with triethyl phosphonoacetate<sup>16</sup> (Horner–Emmons reaction). The carboxylic acids  $8_n$  were quantitatively converted into the corresponding chlorides  $9_n$  with oxalyl chloride in refluxing benzene ( $9_2$ , mp 162 °C;  $9_3$ , waxy compound). These acid chlorides were condensed without purification with the *N*-acetyl- $[\text{18}]\text{-N}_2\text{O}_4$  derivative<sup>17</sup> to give the corresponding diamides  $10_n$  (waxy compounds; 83% yields). Reduction with diborane and subsequent treatment with concentrated  $\text{HCl}$  gave  $M_n$  ( $M_2$ , oil, 92% yield;  $M_3$ , oil, 88% yield).

The  $N,N'$ -diethyl- $[\text{18}]\text{-N}_2\text{O}_4$  macrocycle D (mp 48 °C) was obtained by reduction with diborane of the diacetyl derivative (mp 98 °C) resulting from the condensation (90% yield) of acetyl chloride with the  $[\text{18}]\text{-N}_2\text{O}_4$  macrocycle.

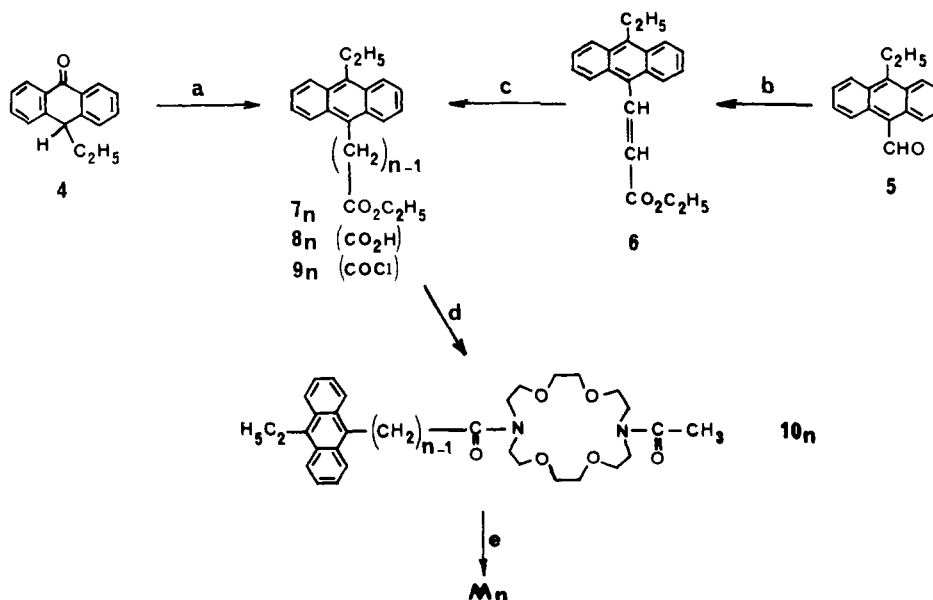
**Characterization of the Free Ligands. (1) Structure of the Anthraceno-Cryptands ( $A_{nn}$ ). (a) X-ray Structure Analysis.** The crystal structures<sup>9b</sup> of the cryptands  $A_{22}$  and  $A_{33}$  show that a preformed cavity exists which should allow internal cation complexation (Figure 1). In the crystalline state, the nitrogen lone

(14) Meyer, K. H.; Schlosser, H. *Justus Liebigs Ann. Chem.* **1920**, 420, 130.

(15) Martin, R. H.; Van Hove, L. *Bull. Soc. Chim. Belg.* **1952**, *61*, 504.

(16) Kosolapoff, G. M. *J. Am. Chem. Soc.* **1946**, *68*, 1103.

(17) Ogata, N.; Sanui, K.; Fujimura, H. *J. Appl. Polym. Sci.* **1981**, *26*, 4149.

Scheme III. Synthesis of the Reference Compounds  $M_n$ <sup>a</sup>

<sup>a</sup> (a) Zn,  $\text{BrCH}_2\text{CO}_2\text{Et}$ , toluene/THF, (b)  $(\text{EtO})_2\text{POCH}_2\text{CO}_2\text{Et}$ , NaH, 1,2-dimethoxyethane; (c)  $\text{H}_2$ , Pd/C, ethanol; (d) *N*-acetyl- $-\text{N}_2\text{O}_4$ ,  $\text{Et}_3\text{N}$ , benzene; (e) (i)  $\text{B}_2\text{H}_6$ /THF, (ii)  $\text{HCl}/\text{H}_2\text{O}$ , (iii)  $\text{LiOH}/\text{H}_2\text{O}$ .

pairs of  $A_{22}$  are oriented, inside the cavity, toward the aromatic ring whereas they point outside for  $A_{33}$ .

(b) **NMR Spectrometry.** The NMR spectra ( $^1\text{H}$  and  $^{13}\text{C}$ ) in solution (methylene chloride, chloroform<sup>9a</sup> and toluene<sup>7</sup>) show that the structure of the free ligands is symmetrical on the NMR time scale and resembles that determined previously by X-ray structure analysis.<sup>9b</sup> In particular, the  $^{13}\text{C}$  NMR spectra indicate that the carbon skeleton of the two cryptands exhibits  $C_{2v}$  symmetry.

(c) **UV-Visible Absorption Spectra.** UV absorption spectra of  $A_{nn}$  in diluted solutions (MCH, MeOH, toluene) are characteristic of 9,10-disubstituted alkyanthracenes. However, they present slight but significant bathochromic and hypochromic shifts in comparison with 9,10-di-*n*-propylanthracene (R) (Figure 2). The UV absorption of the  $[\text{18}]\text{-N}_2\text{O}_4$  chromophore is located at high energy ( $<300$  nm) and its spectral contribution is negligible compared to the  $^1\text{B}_b$  transition of the aromatic moiety. The spectra of the molecules  $M_n$  have the same positions as the reference compound R and no important interactions between the nitrogen lone pairs and the anthracene ring in the ground state are detected by this technique; nevertheless, a hypochromic effect of  $M_n$  compared to R suggests that, on average, the amine and anthracene  $^1\text{L}_a$  transition moments tend to be parallel and superimposed,<sup>18</sup> in a way similar to that in  $A_{nn}$ .

The molar extinction coefficients of compounds  $M_n$  and R are not significantly affected by the nature of the solvent in contrast to those recorded for the macrobicyclic derivatives  $A_{nn}$ , which exhibit a weak but clear variation from toluene to methanol (12–14%) (Table I).

This solvent dependence could be correlated with the well-known ability of cryptands to display several sets of conformers differing by the orientation of the nitrogen lone pairs.<sup>12,19</sup> Indeed we have demonstrated in previous papers<sup>7,9a</sup> that  $A_{22}$  is present as two main conformers in the ground state: an endo–endo form, prevailing in the crystal,<sup>9b</sup> which is in rapid interconversion in fluid solution with an exo–exo form where the lone pairs do not interact with the aromatic  $\pi$  cloud. The relative populations of these two conformers are temperature and solvent dependent; in aprotic solvents, the endo–endo conformer is largely favored (6/1),<sup>7</sup> whereas in a protic solvent such as methanol, the exo–exo species could be predominant due to specific solvation of the nitrogens by the solvent. As a consequence, the UV spectrum is shifted

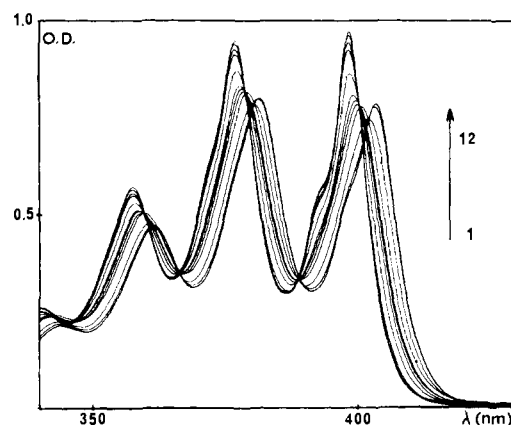


Figure 3. Electronic absorption spectra of  $A_{22}$  in methanol versus  $-\log [\text{H}^+]$  (25 °C).  $[A_{22}] = 1.8 \times 10^{-4}$  M;  $I = 0.1$  (TBA- $\text{ClO}_4$ ) (TBA, tetrabutylammonium).  $-\log [\text{H}^+]$ : 1, 3.57; 2, 5.49; 3, 7.16; 4, 7.54; 5, 8.12; 6, 8.52; 7, 8.71; 8, 8.90; 9, 9.29; 10, 10.02; 11, 11.08; 12, 12.09.

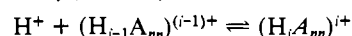
Table II. Protonation Constants of Anthraceno-Cryptands  $A_{22}$  and  $A_{33}$  in Methanol<sup>a</sup>

	ligands			
	$[\text{2.2}]^b$ ( $r = 1.4 \text{ \AA}$ )	$[\text{2.2.2}]^b$ ( $r = 1.4 \text{ \AA}$ )	$A_{22}$ ( $r = 1.1 \text{ \AA}$ ) <sup>c</sup>	$A_{33}$ ( $r = 1.6 \text{ \AA}$ ) <sup>c</sup>
$\log K_1$	$10.64 \pm 0.01$	$10.72 \pm 0.03$	$9.97 \pm 0.03$	$10.79 \pm 0.17$
$\log K_2$	$9.14 \pm 0.01$	$9.03 \pm 0.01$	$8.42 \pm 0.05$	$9.52 \pm 0.27$
$\log K_1 - \log K_2$	$1.20 \pm 0.01$	$1.69 \pm 0.01$	$1.55 \pm 0.06$	$1.27 \pm 0.32$

<sup>a</sup>  $T = 25.0 \pm 0.1$  °C;  $I = 0.1$  (tetrabutylammonium perchlorate). <sup>b</sup> From ref 20a. <sup>c</sup> Radius of the free cavity of  $A_{nn}$  estimated from the crystallographic data.<sup>9b</sup>

toward higher energy. Although the conformational distribution in  $A_{33}$  has not been established, a similar trend may be expected. This interpretation is consistent with the modification of the UV spectra observed in presence of protons. Indeed, the addition of trifluoroacetic acid in excess to the solutions exactly restores the absorption spectrum of the reference compound R by quaternization of the nitrogens.

The constants  $K_i$  ( $i = 1, 2$ ) associated to the equilibria



and corresponding to the protonation of one of the two nitrogen sites of the cryptands have been determined (Table II; Figure 3).

(18) Tinocco, I., Jr. *J. Am. Chem. Soc.* **1960**, *82*, 4785.

(19) Graf, F.; Kintzinger, J.-P.; Lehn, J.-M.; Le Moigne, J. *J. Am. Chem. Soc.* **1982**, *104*, 1672.

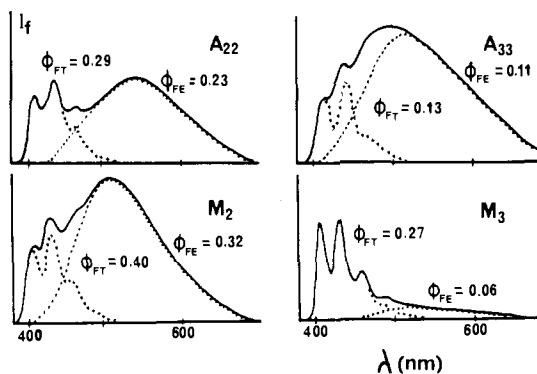


**Figure 4.** Corrected fluorescence emission spectra of R,  $A_{nn}$ , and  $M_n$  in degassed tetrahydrofuran (concentration,  $<10^{-5}$  M) at 20 °C. The exciplex contribution (---) is obtained from difference spectra between  $A_{nn}$  or  $M_n$  (—) and R (+);  $\lambda_{\text{exc}} = 380$  nm.  $\phi_{\text{FT}} = \phi_{\text{FM}} + \phi_{\text{FE}}$ ;  $\phi_{\text{FT}}$ ,  $\phi_{\text{FM}}$  and  $\phi_{\text{FE}}$  are total, monomer-like, and exciplex fluorescence emission quantum yields, respectively.

The  $K_1$  values of the [2.1.1]-, [2.2.1]-, and [2.2.2]cryptands decrease when the cavity size increases; this has been explained by the formation of an in-in monoprotonated species.<sup>20</sup> In the present case, the reverse is observed from  $A_{22}$  to  $A_{33}$  (Table II): monoprotonation of the smaller anthraceno-cryptand  $A_{22}$  is more difficult by  $\sim 1$  order of magnitude as compared to  $A_{33}$ . This may be due to the fact that inside protonation requires a change in bridgehead orientation for  $A_{22}$ , which is preferentially out-out in methanol solution, but not for  $A_{33}$ , which contains at least one in site<sup>21</sup> (vide infra).

The  $\Delta \log K = \log K_1 - \log K_2$  values are known to increase<sup>20</sup> when the cavity size of the cryptand decreases, indicating relative destabilization of the diprotonated species. In agreement with these observed trends,  $\Delta \log K$  is higher for the smaller anthraceno-cryptand  $A_{22}$ . Similarities clearly appear in table II for  $A_{33}$  and [2.2], suggesting a weak participation of the aromatic ring in the protonated species of  $A_{33}$ .

According to the conformational dynamics of the cryptand  $A_{22}$ , it is reasonable to postulate an out-out geometry for the diprotonated species and infer it for  $A_{33}$ . Moreover, this could explain the <sup>1</sup>H NMR spectra of  $A_{22}$  in methanol ( $\text{CD}_3\text{OD}$ ) in the presence of trifluoroacetic acid. Since the NMR data are consistent with a symmetrical structure of the molecular framework (implying the same conformation at the nitrogen sites), they indicate that this structure differs from metal cations to protons. In the presence of metal cations, it has already been demonstrated<sup>9a</sup> that both the nitrogen lone pairs present an "in-in" orientation, and consequently, an "out-out" geometry for the diprotonated  $A_{nn}$  is likely.

**(2) Fluorescence Emission Spectra.** Whereas 9,10-di-*n*-propylanthracene (R) displays the expected emission fluorescence for the anthracenic chromophore (Figure 4), anthracenes bridging an [18]- $\text{N}_2\text{O}_4$  ring ( $A_{nn}$  and  $M_n$ ) exhibit a dual fluorescence, which can be analyzed as follows: a structured part similar to the emission spectrum of the reference compound R ascribable to the locally excited state and a red-shifted structureless band attributed to an intramolecular exciplex involving nitrogen lone pairs and the aromatic ring<sup>4,7,21</sup> (the fluorescence excitation spectra scanned on the structured and the nonstructured bands are identical). The relatively weak intensity of  $A_{33}$  fluorescence emission in methanol is ascribable to the fast formation of the exciplex (in less than 50 ps) and to the easy formation of nonemitting ion pairs.

For compounds  $A_{nn}$  and  $M_n$ , the charge-transfer character of the excited complex has been demonstrated by the red shift of the maximum for exciplex emission as a function of the polarity of the solvent.

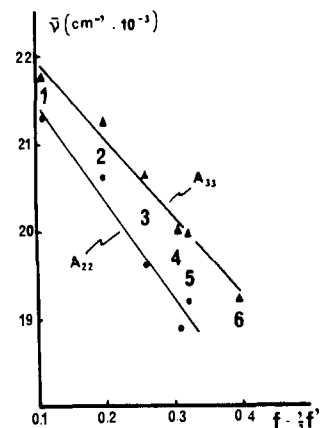


**Figure 5.** Wavenumber of the exciplex emission maximum of  $A_{nn}$  at 20 °C as a function of solvent polarity parameter.  $f^{-1/2}f'$ ;  $f = (\epsilon - 1)/(2\epsilon + 1)$ ;  $f' = (n^2 - 1)/(2n^2 + 1)$ . Solvent ( $f^{-1/2}f'$ ): (1) methylcyclohexane (0.106); (2) trichloroethylene (0.197); (3) diethyl ether (0.256); (4) tetrahydrofuran (0.306); (5) methylene chloride (0.319); (6) methanol (0.391).

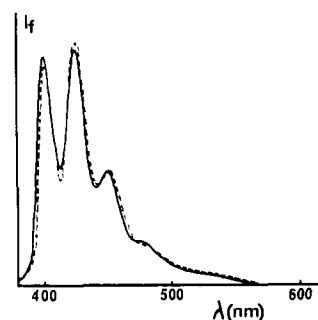


**Figure 6.** Corrected fluorescence emission spectrum of  $A_{22}$  in degassed methanol (—) (concentration  $<10^{-5}$  M) at 20 °C.  $\lambda_{\text{exc}} = 380$  nm ( $\phi_{\text{F}} = 0.68$ ). The major conformer in this solvent is likely to exhibit an exo-exo geometry for the nitrogen lone pairs. The other (minor) conformer (endo-endo) presumably leads directly to an ion pair stabilized by methanol, which does not emit fluorescence. In the presence of an excess of  $\text{CF}_3\text{CO}_2\text{H}$ ,  $\phi_{\text{F}} = 0.80$  (---).

It was argued<sup>7</sup> that the two nitrogens are simultaneously involved in exciplex formation in  $A_{22}$ . A similar geometry should also apply to  $A_{33}$ , as shown by solvatochromic experiments (Figure 5) and supported by the detection of only one exciplex by picosecond time resolved spectroscopy.<sup>21</sup>

In the flexible reference molecules  $M_n$ , the formation of an intramolecular exciplex involving the two nitrogens seems rather unlikely according to the high fluorescence exciplex quantum yields observed [for example in degassed toluene at 20 °C ( $C < 10^{-5}$  M),  $\phi_{\text{FE}} = 0.39$  for  $M_2$  and 0.12 for  $M_3$ ], which do not compare well to known data concerning triple exciplexes in flexible systems.<sup>22</sup> However it cannot be completely discounted.

In methanol, no exciplex is observed with  $A_{22}$ , only a relatively strong monomeric type fluorescence is recorded ( $\phi_{\text{F}} = 0.68$ ). This effect does not appear with the other compounds except to some extent with  $M_3$ , which displays only a weak monomeric emission. The occurrence of a specific solvation of the nitrogen lone pairs of  $A_{22}$  by methanol is assumed to maintain an exo-exo geometry in the excited state, hindering the exciplex formation (Figure 6). The minor conformer (endo-endo) presumably leads, in this protic solvent, to an ion pair that does not emit light.<sup>23</sup>

**Complexation of Cations by Anthraceno-Cryptands  $A_{nn}$  in the Ground State.** The spectroscopic properties of the anthraceno-cryptands are strongly modified in the presence of protons and

(20) (a) Spiess, B.; Arnau-Neu, F.; Schwing-Weill, M. *J. Helv. Chim. Acta* **1979**, *62*, 1531. (b) Lehn, J.-M.; Sauvage, J.-P. *J. Am. Chem. Soc.* **1975**, *97*, 6700.

(21) Fages, F. Thèse d'Etat, Université de Bordeaux I, Talence, France, 1988.

(22) (a) Larson, J. R.; Petrich, J. W.; Yang, N. C. *J. Am. Chem. Soc.* **1982**, *104*, 5000. (b) Yang, N. C.; Gerald, R., II; Wasielewski, M. R. *Ibid.* **1985**, *107*, 5531.

(23) Beens, H.; Weller, A. In *Organic Molecular Photophysics*; Birks, J. B., Ed.; Wiley: London, 1975; Vol. 2, p 159.

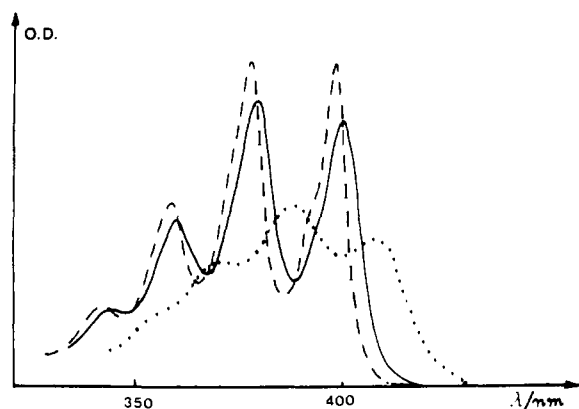


**Figure 7.** Electronic absorption spectrum ( ${}^1L_a$  band, 20 °C) of  $A_{22}$  in methanol (concentration,  $<10^{-4}$  M): —, without salt; ---, with  $KClO_4$  ( $10^{-1}$  M); ···, with  $AgNO_3$  ( $10^{-1}$  M).

**Table III.** UV Spectral Modification (on the  ${}^1L_a$  Band) of  $A_{nn}$  and  $M_n$  ( $\leq 10^{-4}$  M, Methanol, 20 °C) in the Presence of Salts or  $CF_3COOH$  (ca.  $10^{-1}$ – $10^{-2}$  M)<sup>a</sup>

		LiClO <sub>4</sub>	NaClO <sub>4</sub>	KClO <sub>4</sub>	AgClO <sub>4</sub>	TlNO <sub>3</sub>	CF <sub>3</sub> COOH
$\Delta\epsilon$	} $A_{22}$	—	↑9	↑12	↓30	↓19	↑15
$\Delta\lambda$		—	→2	←1	→10	→7	—
$\Delta\epsilon$	} $A_{33}$	—	↓13	↓2	↓28	↓4	↑16
$\Delta\lambda$		—	→1	→1	→4	→2	←1
$\Delta\epsilon$	} $M_2$	*	*	↑5	↑1	↑2	↑6
$\Delta\lambda$		—	—	→1	→1	→3	←2
$\Delta\epsilon$	} $M_3$	*	*	—	↑7	↑2	—
$\Delta\lambda$		—	—	—	→1	→1	—

<sup>a</sup>  $\Delta\epsilon$  represents the variation (%) of the absorption intensity and  $\Delta\lambda$  the shift (nm). Arrows ↑ and ↓ denote hyper- and hypochromism, respectively. Arrows → and ← indicate batho- and hypsochromism respectively. (—) no effect; (\*) not recorded.

of the metal cations examined ( $Li^+$ ,  $Na^+$ , and  $K^+$  perchlorates and  $Ag^+$  and  $Tl^+$  nitrates).

**(1) UV-Visible Absorption Spectroscopy.** The absorption spectra of  $A_{nn}$  but not of R are affected by the addition of  $CF_3COOH$  or of salts (except  $LiClO_4$ ), the perturbation depending on the nature of the added species (Figure 7). Under the same experimental conditions, the spectra of the flexible compounds are only little altered (Table III).

Indeed, with  $M_n$  only weak hyperchromic effects are observed while some hypochromic effects are noticed with  $A_{nn}$ , depending on the nature of the added cation. Moreover, heavy cations, i.e.,  $Ag^+$  and  $Tl^+$ , produce hypochromic and bathochromic shifts (larger with  $A_{22}$ ).

These data are consistent with the formation of complexes between  $A_{nn}$  and the cations (except  $Li^+$ , probably too small to be well complexed) in which the ion is bound to the [18]- $N_2O_4$  ring and held in the vicinity of the  $\pi$  system. This probably explains the red shift of the spectra with  $Ag^+$  and  $Tl^+$ , which points to a ground-state complex between the ions and the aromatic ring.

**(2) Stoichiometry and Stability Constants of the Complexes.** The electronic spectra and the stability constants of the Tl(I) and Ag(I) (1:1) complexes formed with  $A_{22}$  (Figure 8) and  $A_{33}$  (Table IV) in methanol have been determined by simultaneous potentiometric and spectrophotometric measurements. The data have been processed by the LETAGROP-SPEFO program.<sup>24</sup>

Though the cavity size of the cryptand  $A_{22}$  seems compatible with the ionic radius of the Ag(I) cation, the stability constant of the  $[Ag^+ \subset A_{22}]$  cryptate decreases as compared to  $[Ag^+ \subset 2.2]$

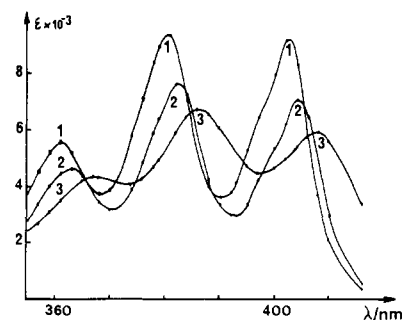


**Figure 8.** Calculated electronic absorption spectra of  $A_{22}$  and its Tl(I) and Ag(I) complexes in methanol. 1,  $A_{22}$ ; 2,  $[Tl^+ \subset A_{22}]$ ; 3,  $[Ag^+ \subset A_{22}]$ .

**Table IV.** Stability Constants of Thallium(I) and Silver(I) Complexes Formed with the Anthraceno-Cryptands  $A_{22}$  and  $A_{33}$  in Methanol<sup>a</sup>

ligands	$\log K_s$			
	[2.2] ( $r = 1.4$ Å)	[2.2.2] ( $r = 1.4$ Å)	$A_{22}$ ( $r = 1.1$ Å)	$A_{33}$ ( $r = 1.6$ Å)
$Tl^+$ ( $r_i = 1.49$ Å)	3.54 <sup>b</sup>	10.10 <sup>c</sup> 9.10 <sup>d</sup>	8.52	7.07
$Ag^+$ ( $r_i = 1.13$ Å)	10.02 <sup>e</sup> 10.18 <sup>b</sup>	12.30 <sup>h</sup> 12.22 <sup>g</sup>	9.51	9.36

<sup>a</sup>  $T = 25.0 \pm 0.1$  °C;  $I = 0.1$  (tetrabutylammonium perchlorate). The accuracy of our results is 0.05 for  $\log K_s$  and is equal to  $2\sigma$ .  $r_i$ , ionic radius of cations;<sup>31</sup>  $r$ , radius of the cavity of the coronand or cryptand; the latter was estimated from crystallographic data.<sup>9b</sup> <sup>b</sup> Cox, B. G.; Firman, P.; Horst, H.; Schneider, H. *Tetrahedron* **1983**, *39*, 343. <sup>c</sup> Yee, E. L.; Tabib, J.; Weaver, M. J. *J. Electroanal. Chem.* **1979**, *96*, 241. <sup>d</sup> Spiess, B., Thèse de doctorat d'Etat, Université Louis Pasteur, Strasbourg, France, 1981. <sup>e</sup> Cox, B. C.; Schneider, H.; Schulz, H.; Stroka, J. *J. Am. Chem. Soc.* **1978**, *100*, 4746. <sup>f</sup> Gutknecht, H.; Schneider, H.; Stroka, H. *Inorg. Chem.* **1978**, *17*, 3327. <sup>g</sup> Buschmann, H. *J. Inorg. Chim. Acta* **1985**, *102*, 95. <sup>h</sup> Lejaille, M. F.; Livertoux, M.; Guidon, C.; Bessière, J. *Bull. Soc. Chim. Fr.* **1978**, 373.

and  $[Ag^+ \subset 2.2.2]$  cryptates (Table IV). The loss of two coordination sites in [2.2],  $A_{22}$ , and  $A_{33}$  silver(I) complexes induces a decrease in stability constants of at least 2 orders of magnitude, as compared to  $[Ag^+ \subset 2.2.2]$  in the same solvent. In addition, the deformation of the cavity by the aromatic groups may also contribute in particular by increasing the distance between the bridgehead nitrogens, which are expected to be the preferred coordination sites of the  $Ag^+$  ions.

Similarly, for the  $A_{22}$  and  $A_{33}$  thallium(I) cryptates compared to  $[Tl^+ \subset 2.2.2]$ , a decrease of at least 1 order of magnitude of the stability constant is found (Table IV). In order to analyze the above trend, it is appropriate to compare the stability of  $K^+$  complexes with two macrobicyclic ligands [2.2.2] ( $\log K_s = 8.7$ ; Table IV, footnote h) and [2.2.C<sub>8</sub>] ( $\log K_s = 5.2^{20b}$ ) in methanol. In the latter case, the loss of stability is  $\sim 3$  orders of magnitude for the complex formed with the cryptand with the hydrocarbon chain [2.2.C<sub>8</sub>]. It appears that the loss in stability of the  $A_{22}$  thallium(I) complex compared to  $[Tl^+ \subset 2.2.2]$  is substantially smaller than the stability decreases between [2.2.2] and [2.2.C<sub>8</sub>]  $K^+$  complexes, in spite of the deformation of the cavity of  $A_{22}$ . A stabilization effect by the anthracene moiety of the thallium(I)  $A_{22}$  complex is observed here, in agreement with NMR emission fluorescence and X-ray structure data,<sup>9a,b</sup> which have shown that the cation  $Tl^+$  is inside the cavity, coordinated by the oxygen and nitrogen atoms of the ligand and in interaction with the aromatic ring.

**(3)  ${}^1H$  and  ${}^{13}C$  NMR Spectroscopy.** NMR spectra ( $D_2Cl_2$ ,  $DCCl_3$ , toluene) were recorded for cryptands  $A_{nn}$  in the absence and in the presence of cations ( $K^+$ ,  $Tl^+$ ,  $Ag^+$ ). The detailed analysis of the spectra was reported elsewhere.<sup>7,9a</sup>

From this study, it emerges that the addition of an excess of salts ( $K^+$ ,  $Ag^+$ ,  $Tl^+$ ) to the solutions of  $A_{nn}$  is followed by a marked modification of the spectra (Figure 9) indicative of an important conformation reorganization showing that the cation is inside the cavity.

All the  ${}^1H$  NMR patterns appear to be affected in a similar way by the three cations, which induce a deshielding of the

(24) Sillen, L. G.; Warnquist, B. *Ark. Kemi* **1968**, *31*, 315, 377.

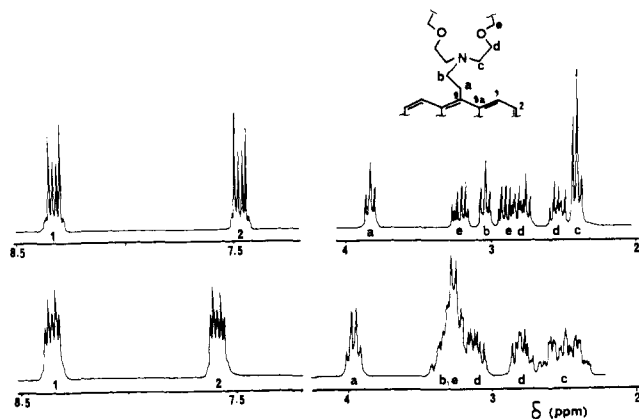


Figure 9. 200-MHz  $^1\text{H}$  NMR spectra of  $\text{A}_{22}$  in  $\text{CDCl}_3$  at room temperature. Top: without salt. Bottom: with  $\text{TiNO}_3$  (saturated solution).

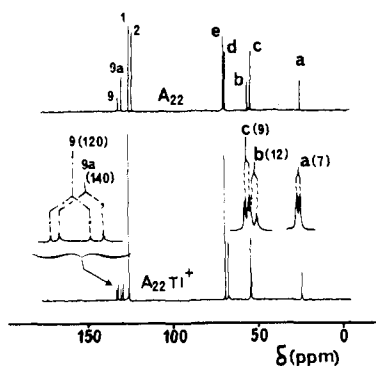


Figure 10. 50-MHz  $^{13}\text{C}$  NMR spectra of  $\text{A}_{22}$  in  $\text{CDCl}_3$  at room temperature. Top: without salt. Bottom: with  $\text{TiNO}_3$  (saturated solution). The coupling constants ( $J_{\text{Ti}-\text{C}}$ ) (hertz) are given in parentheses.

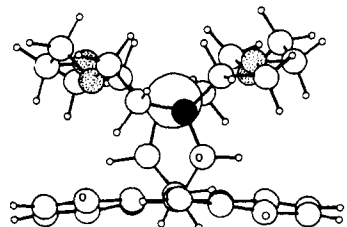


Figure 11. Molecular structure of  $\text{Ti}^+ - \text{A}_{22}$  complex along the short axis of the anthracene ring. Note the deformation of the aromatic nucleus. The distance between  $\text{Ti}^+$  and the average plane of the aromatic ring is 3.2 Å.

aromatic and benzylic signals. Analogous trends were noted<sup>9a</sup> in the  $^{13}\text{C}$  NMR spectra.

The results obtained with  $\text{Ti}^+$  must be emphasized; indeed coupling constants between the cation and H and C nuclei of the aliphatic part (3–14 Hz) of the ligand  $\text{A}_{22}$  appear in line with earlier data reported<sup>25</sup> for [2]cryptates. Moreover, coupling constants (120–140 Hz) between  $\text{Ti}^+$  and aromatic carbons of the central ring were observed for the first time; they are evidence of some bonding between the cation and the anthracene ring and thus of the insertion of the cation inside the cavity (Figure 10). No perturbation of the spectra of R was detected in the presence of  $\text{Ti}^+$ .

With  $\text{A}_{33}$ , the coupling constants are not easy to determine (at room temperature the signals broaden); probably the size of the cavity is too large to keep the cation tightly in a definite position. Further, for the flexible opened molecule ( $\text{M}_2$ ), no coupling was observed between the protons and the  $\text{Ti}^+$  nucleus; only a deshielding of the signals of the aliphatic protons was detected when adding a large excess of  $\text{TiNO}_3$  to the solutions.

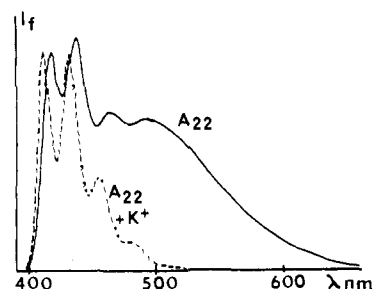


Figure 12. Corrected fluorescence emission spectra of  $\text{A}_{22}$  in degassed  $\text{CH}_2\text{Cl}_2$  (concentration,  $<10^{-6}$  M,  $\lambda_{\text{exc}}$ , 380 nm, 20 °C). —, without salt; ---, with  $\text{KClO}_4$  (saturated solution).

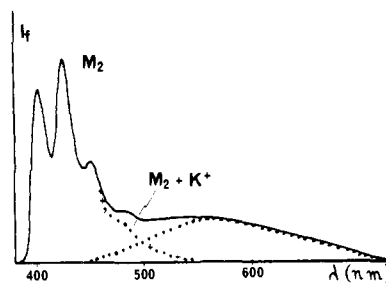


Figure 13. Corrected fluorescence emission spectra of  $\text{M}_2$  in nondegassed methanol ( $10^{-6}$  M,  $\lambda_{\text{exc}}$ , 380 nm, 20 °C). —, without salt; + with  $\text{KClO}_4$  (saturated solution); ···, the fluorescence exciplex spectrum.

Table V. Fluorescence Quantum Yields of  $\text{A}_{nn}$ ,  $\text{M}_n$ , and R in Methanol (concentration,  $<10^{-5}$  M, 20 °C,  $\lambda_{\text{exc}}$ , 380 nm) in the Absence and the Presence of Salts or  $\text{CF}_3\text{CO}_2\text{H}$  ( $<10^{-2}$  M)

	none	$\text{LiClO}_4$	$\text{NaClO}_4$	$\text{KClO}_4$	$\text{AgClO}_4$	$\text{TiNO}_3$	$\text{CF}_3\text{CO}_2\text{H}$
$\text{A}_{22}$	0.68	0.70	0.57	0.64	0.05	0.05	0.80
$\text{A}_{33}$	0.04 <sup>a</sup>	0.05 <sup>a</sup>	0.17	0.30	0.23 <sup>a</sup>	0.07	0.70
$\text{M}_2^d$	0.10 <sup>a</sup>	c	c	0.31	0.31	0.29	0.50
$\text{M}_3^d$	0.26	c	c	0.50	0.26	0.46	0.53
R	0.76	b	b	b	0.39	0.67	b

<sup>a</sup> Dual fluorescence emission. <sup>b</sup> No effect observed. <sup>c</sup> Not measured. <sup>d</sup> Nondegassed.

(4) Structure of the  $\text{TiNO}_3 - \text{A}_{22}$  Complex ( $[\text{Ti}^+ \subset \text{A}_{22}]$ ,  $\text{NO}_3^-$ ). Monocrystals of  $\text{Ti}^+ \cdot \text{A}_{22}$  complex were obtained from chloroformic solution of  $\text{A}_{22}$  saturated with  $\text{TiNO}_3$  and the structure was determined by X-ray crystallography.<sup>9a</sup> As expected from spectroscopic measurements,  $\text{Ti}^+$  is encaged inside the cryptand (Figure 11) and coordinated with the oxygen and nitrogen atoms as well as the aromatic ring<sup>9a,c</sup> ( $\text{Ti}^+ \cdots \text{anthracene} = 3.2$  Å). From examination of the NMR and UV spectra of the 1:1 complexes of  $\text{A}_{nn}$  with the other cations, it is deduced that they are also inclusion complexes.

(5) Fluorescence Emission Spectra. (a) Light-Metal Cations. Addition of complexable cations ( $\text{Na}^+$ ,  $\text{K}^+$ ) to the solution of  $\text{A}_{nn}$  (protic or aprotic solvents) strongly reduces the red-shifted emission (exciplex component) and increases distinctly the intensity of the structured spectral part (Figure 12); no effect was detected with  $\text{Li}^+$  (Table V). Thus involvement of the nitrogen sites in complexation is beyond doubt, since complexation prevents or strongly reduces the amine–anthracene exciplex formation.

Similar trends are observed with the flexible models  $\text{M}_n$  (Figure 13) where the cation is expected to be crowned by the [18]- $\text{N}_2\text{O}_4$  macrocycle and so hinders the intramolecular exciplex formation. Under the same experimental conditions, no spectral modifications were detected with R. Gradual addition of cations to  $\text{A}_{nn}$  solutions results in a progressive increase of the fluorescence intensity as shown in Figure 14. The resulting titration curves point to a 1:1 stoichiometry for the complex. Thus, compounds  $\text{A}_{nn}$ , especially  $\text{A}_{33}$  whose fluorescence emission was of low intensity, undergo a spectacular increase of light emission by addition of salts in the manner of a lamp that rekindles by addition of oil. These observations are in line with other recent results.<sup>1</sup>

(25) Lehn, J.-M.; Sauvage, J.-P.; Dietrich, B. *J. Am. Chem. Soc.* 1970, 92, 2916.

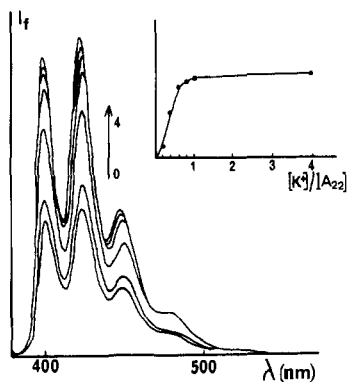


**Figure 14.** Fluorescence emission intensity of compound  $A_{22}$  ( $10^{-5}$  M) in nondegassed methanol as a function of added  $KClO_4$  ( $20^\circ C$ ,  $\lambda_{exc}$ , 380 nm).  $KClO_4$  ( $10^{-5}$  M): 0.0, 0.2, 0.4, 0.6, 0.8, 1.0, and 4.0. The titration curve  $I_f \propto [K^+]$  points to a 1:1 stoichiometry for  $[K^+ \subset A_{22}]$  (Inset).

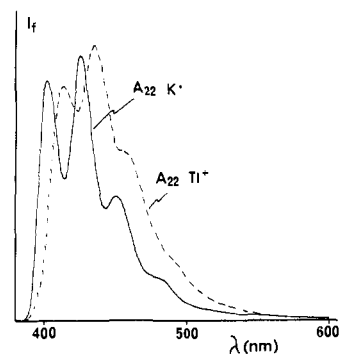


**Figure 15.** Corrected fluorescence emission spectra of  $A_{22}$  in degassed methanol (concentration,  $<10^{-5}$  M,  $\lambda_{exc}$ , 380 nm,  $20^\circ C$ ) in the presence of  $K^+$  ( $10^{-2}$  M) (—) and  $Tl^+$  (---).

**(b) Heavy-Metal Cations.** In contrast to protons and alkali-metal cations,  $Ag^+$  and  $Tl^+$  behave as fluorescence quenchers, especially for  $A_{22}$  (Table V) (cation concentration  $\sim 1000$  fold in excess). If the reference compound R also undergoes a fluorescence quenching by the classical heavy-atom effect, which increases intersystem crossing ( $S_1 \rightarrow T_2$ ), the effect is not so important under the same experimental conditions (Table V). The flexible reference compounds  $M_n$  exhibit a fluorescence quenching intermediate between that of  $A_{nn}$  and R; this is accompanied by the disappearance of exciplex emission, in connection to the complexation of  $Ag^+$  and  $Tl^+$  by the [18]- $N_2O_4$  unit; the quenching is less intense than for  $A_{nn}$  as the average distance between the cation and the anthracene ring is greater.

The fluorescence emission spectra of  $A_{nn}$  in the presence of these two heavy cations was given special attention.

**(c) Thallium Cations ( $Tl^+$ ).** If the fluorescence spectrum of  $A_{22}$  with  $Tl^+$  is a structured anthracene monomer type emission,<sup>9a,c</sup> it is not superimposable to the spectra displayed by the light-cation cryptates (i.e.,  $[K^+ \subset A_{22}]$ ) since a red shift of  $\sim 730$   $cm^{-1}$  was measured (Figure 15). As the excitation fluorescence spectrum well matches the absorption spectrum of the species  $[Tl^+ \subset A_{22}]$ , it was concluded<sup>9a,21</sup> that the emission originates from an excited  $[Tl(I):anthracene]$  complex preformed in the ground state. Interestingly, only a few weak complexes between  $Tl^+$  and arenes<sup>26</sup> are known in the crystalline state; this anthraceno-cryptand  $A_{22}$  appears well suited for revealing and studying this kind of faint interaction even in fluid solutions. With  $A_{33}$ , the fluorescence emission is close to that observed with light cations, probably as a consequence of the larger size of the cavity, in agreement with NMR measurements and UV spectroscopy.<sup>9a</sup> The anthraceno crown ethers  $M_n$  behave as  $A_{33}$  in presence of  $Tl^+$ .

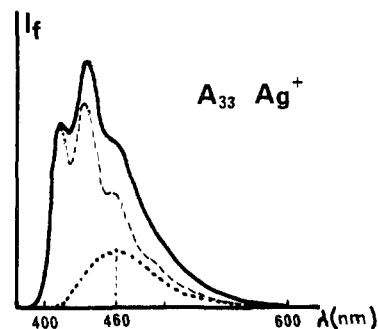
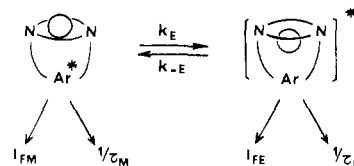


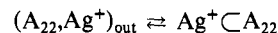
**Figure 16.** Corrected fluorescence emission spectra of  $A_{33}$  in degassed methanol (concentration,  $<10^{-5}$  M,  $\lambda_{exc}$ , 380 nm,  $20^\circ C$ ) in the presence ( $10^{-2}$  M) of  $AgNO_3$  (—) and  $NaClO_4$  (---). (···) represents the fluorescence exciplex spectrum.

#### Scheme IV<sup>a</sup>



<sup>a</sup>  $k_E$  and  $k_{-E}$  are the rate constants for exciplex formation and dissociation, respectively.  $\tau_M$  and  $\tau_E$  are the fluorescence lifetimes of locally excited  $^1A^*$  (without any interaction with the nitrogen lone pairs or  $Ag^+$ ) denoted "monomer" and of the exciplex ( $Ag^+ \cdot A_{33}$ ), respectively. At  $20^\circ C$ ,  $k_E = 1.9 \times 10^8$   $s^{-1}$ ;  $1/\tau_E = 2.1 \times 10^8$   $s^{-1}$ ;  $\Delta G^\circ(M \rightarrow E) = -0.37$  kcal  $mol^{-1}$ .

**(d) Silver Cations ( $Ag^+$ ).** The solutions of  $A_{22}$  containing  $Ag^+$  only display a pure monomeric type fluorescence emission spectrum as with the reference compound R or  $A_{22}$  with light cations. The excitation spectrum (scanned at all the wavelengths) fits well with the absorption spectrum of the reference compound R and not with that of a solution of  $A_{22}$  with  $AgNO_3$ . This means that the ground-state charge-transfer complex  $[Ag(I):anthracene]$  does not emit light and that emission originates from a nonperturbed anthracene chromophore. These results are presumably ascribable to the presence of two ground-state complexes: the major one with  $Ag^+$  inside the cavity, forming a nonfluorescent charge-transfer complex, and the minor one with  $Ag^+$  externally bound to the diaza-crown and also partially solvated by  $NO_3$  or  $CH_3OH$ ; because the silver cation is remote from the anthracene ring, the latter complex emits a fluorescence similar to that of R.



In contrast, the fluorescence emission spectrum of  $A_{33}, Ag^+$  solutions is not superposable with those recorded with light cations (i.e.,  $Na^+$  and  $K^+$ ) (Figure 16). By subtraction of the degassed methanol solution spectrum of  $A_{33}, Na^+$  from that of  $A_{22}, Ag^+$ , a nonstructured band peaking at 460 nm emerges. The excitation spectra independent of the wavelength of observation match the absorption spectrum of  $A_{33}, Ag^+$ , underlining the common origin of both emissions. The nonstructured emission band (which disappears in the presence of  $O_2$ ) is postulated to arise from an exciplex between  $Ag^+$  and anthracene. Up to now, only perylene has been reported<sup>27</sup> to form an exciplex with  $Ag^+$ .

The occurrence of an exciplex is fully confirmed by the analysis of the fluorescence emission decays, provided the classical Birks' scheme applies<sup>28</sup> (Scheme IV).

The experimental time dependence of the monomer  $I_M(t)$  and exciplex ( $I_E(t)$ ) fluorescence intensity is found to be given by the following expressions:

(26) (a) Strauss, S. H.; Nolrot, M. D.; Anderson, O. P. *Inorg. Chem.* **1986**, *25*, 3851. (b) Schmidbauer, H.; Hager, R.; Huben, B.; Müller, G. *Angew. Chem., Int. Ed. Engl.* **1987**, *26*, 338 and references therein.

(27) (a) Läufer, A. G. E.; Dreeskamp, H.; Zachariasse, K. A. *Chem. Phys. Lett.* **1985**, *121*, 523. (b) Läufer, A. G. E.; Dreeskamp, H. *Ber. Bunsen-Ges. Phys. Chem.* **1986**, *90*, 1195.

(28) Birks, J. B. *Photophysics of Aromatic Molecules*; Wiley-Interscience: London, 1970.

$$\lambda_{\text{obs}}(405 \text{ nm}) \quad I_M(t) \propto 0.26 \exp(-t/2.36 \text{ ns}) + 0.40 \exp(-t/6.82 \text{ ns})$$

$$\lambda_{\text{obs}}(510 \text{ nm}) \quad I_E(t) \propto -0.25 \exp(-t/2.23 \text{ ns}) + 0.77 \exp(-t/6.46 \text{ ns})$$

The exciplex fluorescence response function (at 510 nm) clearly grows from zero, as shown by the negative value of the first preexponential term. The fact that the sum of preexponential terms of the exciplex decay has a positive value (+0.52) and is not equal to zero, as required within the context of the proposed kinetic scheme, is caused by the presence of "monomer" emission at the observation wavelength (510 nm; see Figure 16). It should be noted that the lifetime values are similar for both monomer and exciplex decays. These observations confirm that the kinetic scheme correctly describes the proposed mechanism of the fluorescent properties of  $A_{33}$  with  $\text{Ag}^+$ .

From the values of the decay parameters and the monomer amplitude ratio, the rate constants appearing in the proposed scheme can be calculated (taking  $\tau_M = 14$  ns, the lifetime of  $A^*$  obtained with  $A_{33}$  in the presence of  $\text{Na}^+$  or  $\text{K}^+$ ). The following rate parameters were obtained at 20 °C:

$$k_E = 1.9 \times 10^8 \text{ s}^{-1} \quad k_{-E} = 1.0 \times 10^8 \text{ s}^{-1} \\ 1/\tau_E = 2.1 \times 10^8 \text{ s}^{-1}$$

leading to

$$\Delta G^\circ = -0.37 \text{ kcal/mol}$$

A more detailed study of the thermodynamics and kinetics of the exciplex formation is under investigation.

## Conclusion

We have prepared a new class of macrobicyclic photoactive ligands, the anthraceno-cryptands  $A_m$ , in which the anthracene nucleus bridges an [18]- $\text{N}_2\text{O}_4$  macrocycle. These molecules display a dual fluorescence (monomer and exciplex) resulting from the intramolecular interaction between the nitrogen lone pairs and the  $\pi$  system. The fluorescence of these compounds was shown to be very sensitive to the solvent and the presence of metal cations. Protic solvents, such as methanol, can induce hydrogen bonds with the nitrogens, relieving the intramolecular nitrogen-anthracene interaction; the solvation is followed by a net enhancement of the monomer emission. Cations that enter into the cavity of  $A_m$  form stable 1:1 cryptates, the cations being held near the aromatic ring. The nitrogen lone pairs, found to quench the singlet excited state of the free ligands, are involved in the complexation of the cation inducing a strong increase of the fluorescence intensity (light cations) with the disappearance of the exciplex component. *These phenomena are dependent on the nature of the cation.* Unusual interactions between heavy-metal cations and the central ring of anthracene have been discovered with these chelators,  $\text{Tl}^+$  leading with  $A_{22}$  to a complex presenting novel interactions and  $\text{Ag}^+$  to a fluorescent exciplex with  $A_{33}$ .

## Experimental Section

Chemicals and solvents (spectrometric grade) were used directly as received. Proton magnetic resonance spectra were recorded on a Bruker AC200 (200 MHz) spectrometer in  $\text{CDCl}_3$ ,  $\text{CD}_2\text{Cl}_2$ ,  $\text{CD}_3\text{OD}$ , and toluene- $d_6$  and on a Perkin-Elmer R24B spectrometer in  $\text{CDCl}_3$  and  $\text{CCl}_4$ . The chemical shifts are given in  $\delta$  values from  $\text{Me}_4\text{Si}$ . UV absorption spectra were recorded on a Cary 219 spectrophotometer at 25 °C. The IR spectrometer was a Perkin-Elmer 1420, and the mass spectrometer an VG Micromass Model 70-70. Fluorescence spectra were obtained with a Hitachi Perkin Elmer MPF44 fluorometer, corrected for emission. The fluorescence quantum yields were determined by comparison with quinine sulfate in 1 N sulfuric acid,<sup>29</sup> and the fluorescence lifetimes were measured by single-photon counting using an Applied Photophysics apparatus as already described.<sup>30</sup> The purity of all new compounds was checked by TLC (silica gel). Ionic cation radii (Å) were taken from ref

31:  $\text{Li}^+$  (0.78),  $\text{Na}^+$  (0.98),  $\text{K}^+$  (1.33),  $\text{Tl}^+$  (1.49),  $\text{Ag}^+$  (1.13).

The thermodynamic constants and the electronic spectra of the different species were determined by simultaneous potentiometric and spectrophotometric measurements. Anthraceno-cryptands solutions ( $10^{-4}$  M), in the presence or absence of  $\text{Ag}(\text{I})$  and  $\text{Tl}(\text{I})$ , were acidified with  $\text{HClO}_4$  (Merck, per anal., 70%) up to  $3 \times 10^{-3}$  M and tetrabutylammonium methoxide (Merck, 25% in methanol) was added progressively. A small sample (500  $\mu\text{L}$ ) was taken after each addition in order to record the absorption spectrum on a Kontron Uvikon 860 spectrophotometer. The  $-\log[\text{H}^+]$  values were measured with a combined glass electrode (Tacussel, High Alkalinity), in which the reference electrode ( $\text{Ag}/\text{AgCl}$ ) was filled with tetrabutylammonium chloride ( $5 \times 10^{-2}$  M) and tetrabutylammonium perchlorate ( $5 \times 10^{-2}$  M) in methanol. Potential differences were measured with a Tacussel Isis 20 000 millivoltmeter. The spectrophotometric and potentiometric data were processed by the program LETAGROP-SPEFO.<sup>24</sup> The range of  $-\log[\text{H}^+]$  used in the experiments was from 3 to 14 for the free ligands and for the thallium complexes and from 3 to 10 for the silver complexes. The metal ( $\text{TlNO}_3$  and  $\text{AgNO}_3$ , Merck per anal.) concentrations were 3-fold in excess with respect to the anthraceno-cryptands concentrations. The ionic strength was maintained constant with tetrabutylammonium perchlorate, 0.1 M.

**2,13-Dioxo-6,9,17,20-tetraoxa-3,12-diaza[14.8<sup>3,12</sup>](9,10)-anthracenophane (3<sub>22</sub>).** To 1.5 L of stirred and degassed benzene were added simultaneously and dropwise at room temperature (8 h) under high dilution conditions two degassed benzenic solutions (2  $\times$  500 mL) of 9,10-anthracenediacetyl dichloride<sup>11</sup> (2.8 g, 9 mmol) and of the [18]- $\text{N}_2\text{O}_4$  macrocycle (2.0 g, 8 mmol) with triethylamine (1.9 g, 19 mmol). After the addition was completed, the mixture was filtered and the solvent removed under reduced pressure. Chromatography on alumina column ( $\text{CH}_2\text{Cl}_2$  as eluent) of the solid brown crude product gave 3<sub>22</sub> as a yellow solid (2.4 g, 61% yield): mp >260 °C;  $^1\text{H NMR}$   $\delta$  2.4–4.1 (m, 24 H, " $\text{N}_2\text{O}_4$ " ring), 4.5–5.1 (AB, 4 H,  $J = 16$  Hz,  $\text{ArCH}_2\text{CO}$ ), 7.5–8.8 (m, 8 H, Ar); IR (KBr pellets) 2940, 2860, 1630, 1470, 1450, 1410, 1120, 1080, 780, 745  $\text{cm}^{-1}$ ; MS  $m/z$  520 (calcd 520). Anal. Calcd for  $\text{C}_{30}\text{H}_{36}\text{N}_2\text{O}_6$ : C, 69.21; H, 6.97; N, 5.38; O, 18.44. Found: C, 68.15; H, 6.91; N, 5.38; O, 18.22.

**3,14-Dioxo-7,10,19,22-tetraoxa-4,13-diaza[16.8<sup>4,13</sup>](9,10)-anthracenophane (3<sub>33</sub>).** By the same procedure as above, using 1.0 g (4 mmol) of [18]- $\text{N}_2\text{O}_4$  macrocycle (2.0 mmol) of triethylamine, and 1.5 g (4.6 mmol) of 9,10-anthracenedipropionyl dichloride,<sup>11</sup> 3<sub>33</sub> was obtained as a yellow solid (1.4 g, 65%): mp >260 °C;  $^1\text{H NMR}$   $\delta$  3.0–4.0 (m, 32 H, " $\text{N}_2\text{O}_4$ " ring,  $\text{ArCH}_2\text{CH}_2\text{CO}$ ), 7.2–8.3 (m, 8 H, Ar); IR (KBr pellets) 2950, 2840, 1630, 1450, 1430, 1410, 1110, 750  $\text{cm}^{-1}$ ; MS  $m/z$  548 (calcd 548). Anal. Calcd for  $\text{C}_{32}\text{H}_{40}\text{N}_2\text{O}_6$ : C, 70.05; H, 7.35. Found: C, 70.13; H, 7.26.

**6,9,17,20-Tetraoxa-3,12-diaza[14.8<sup>3,12</sup>](9,10)anthracenophane (A<sub>22</sub>).** A solution of the diamide 3<sub>22</sub> (0.52 g, 1 mmol) in 30 mL of anhydrous tetrahydrofuran (THF) was placed under nitrogen atmosphere in a 100-mL two-neck flask equipped with a reflux condenser and a serum cap; 5 mL of a solution of diborane (1 M in THF) was added with a syringe. The mixture was stirred and refluxed for 2 h. After cooling to room temperature, distilled water was added cautiously. The solvent was evaporated and the crude amine borane derivative (mp >260 °C, pale yellow powder) obtained was used for the next step without further purification. This solid was treated under  $\text{N}_2$  atmosphere with 10 mL of  $\text{HCl}$  (6 N) at 100 °C for 5 h, after which the solution was cooled to room temperature and 100 mL of distilled water was added. The aqueous layer was made alkaline (pH = 8–9) by addition of  $\text{LiOH}$  (30%) and extracted with 3  $\times$  50 mL of  $\text{CHCl}_3$ . The combined chloroform extracts were dried ( $\text{MgSO}_4$ ) and evaporated to give a brown solid material, which was purified by chromatography on neutral alumina (Merck II-III, eluent  $\text{CH}_2\text{Cl}_2$ ). The pale yellow solid was crystallized in toluene (65%): mp > 260 °C;  $^1\text{H NMR}$   $\delta$  2.40 (m, 8 H,  $\text{NCH}_2\text{CH}_2\text{O}$ ), 2.53–2.77 (m, 8 H,  $\text{NCH}_2\text{CH}_2\text{O}$ ), 3.05 (m, 8 H,  $\text{OCH}_2\text{CH}_2\text{O}$ ), 3.05 ("t", 4 H,  $\text{NCH}_2\text{CH}_2\text{Ar}$ ), 3.83 (m, 4 H,  $\text{CH}_2\text{Ar}$ ), 7.48–8.31 (m, 8 H, Ar); IR (KBr pellets) 2830, 2760, 1600, 1450, 1425, 1340, 1285, 1260, 1240, 1120, 1110, 1080, 1060, 1010, 950, 820, 750, 730, 660, 640  $\text{cm}^{-1}$ ; MS  $m/z$  492 (calcd 492). Anal. Calcd for  $\text{C}_{30}\text{H}_{40}\text{N}_2\text{O}_4$ : C, 73.14; H, 8.18; N, 5.69; O, 12.99. Found: C, 72.44; H, 8.22; N, 5.63; O, 13.01.

**7,10,19,22-Tetraoxa-4,13-diaza[16.8<sup>4,13</sup>](9,10)anthracenophane (A<sub>33</sub>).** Similarly, A<sub>33</sub> was prepared from the diamide 3<sub>33</sub>. A<sub>33</sub> was isolated by neutral alumina chromatography ( $\text{CH}_2\text{Cl}_2$ ) and crystallization in toluene as a yellow solid (77%): mp 215 °C;  $^1\text{H NMR}$   $\delta$  2.09 (m, 4 H,  $\text{ArCH}_2\text{CH}_2\text{CH}_2\text{N}$ ), 2.38 (m, 8 H,  $\text{NCH}_2\text{CH}_2\text{O}$ ), 2.41 (m, 4 H,  $\text{ArCH}_2\text{CH}_2\text{CH}_2\text{N}$ ), 2.85 (m, 8 H,  $\text{NCH}_2\text{CH}_2\text{O}$ ), 3.08 (m, 8 H,  $\text{OCH}_2\text{CH}_2\text{O}$ ), 3.77 ("t", 4 H,  $\text{ArCH}_2$ ), 7.51–8.40 (m, 8 H, Ar); IR (KBr pellets) 3040, 2920, 2860, 1620, 1470, 1445, 1360, 1335, 1315, 1250,

(29) Hanai, S.; Hirayama, F. *J. Phys. Chem.* **1983**, *87*, 83, and references therein.

(30) Desvergne, J.-P.; Bitit, N.; Castellan, A.; Bouas-Laurent, H.; Soullignac, J.-C. *J. Lumin.* **1987**, *37*, 175.

(31) *Handbook of Chemistry and Physics*, 49th ed.; CRC: Cleveland, OH, 1968–1969.



1140, 1110, 1010, 910, 780, 750, 660  $\text{cm}^{-1}$ ; MS  $m/z$  520 (calcd 520). Anal. Calcd for  $\text{C}_{32}\text{H}_{44}\text{N}_2\text{O}_4 \cdot \frac{1}{2}\text{H}_2\text{O}$ : C, 72.45; H, 8.49; N, 5.28; O, 13.58. Found: C, 72.88; H, 8.32; N, 5.28; O, 13.54.

**9-[(Ethoxycarbonyl)methyl]-10-ethylanthracene (7<sub>2</sub>).** To a stirred suspension of zinc powder (6.5 g, 0.1 mol) in dried THF (150 mL) was added ethyl bromoacetate (17 g, 0.1 mol) dropwise under  $\text{N}_2$  atmosphere. After completion of the operation, a small amount of iodine was added; then the reacting medium was refluxed and 10-ethylanthrone<sup>14</sup> (4.5 g, 20 mmol) dissolved in THF-toluene (1/1 v/v; 100 mL) was added dropwise. Reflux was continued for 2 h; concentrated  $\text{H}_2\text{SO}_4$  (5 mL) was added and reflux was maintained 1 h longer. After being cooled to room temperature, the mixture was hydrolyzed with acidic water (10%  $\text{H}_2\text{SO}_4$ , 500 mL). The usual workup was followed by chromatography on an  $\text{SiO}_2$  column (eluent ligroin), and 7<sub>2</sub> was obtained (4.7 g, 80%) as yellow pale crystals: mp 88–89 °C;  $^1\text{H NMR}$   $\delta$  0.80–1.50 (2 t, 6 H,  $\text{CH}_3\text{C}-\text{H}_2\text{OCO}$ ,  $\text{CH}_3\text{CH}_2\text{Ar}$ ), 3.40 (q, 2 H,  $\text{CH}_3\text{CH}_2\text{Ar}$ ), 3.90 (q, 2 H,  $\text{CH}_3\text{CH}_2\text{OCO}$ ), 4.30 (s, 2 H,  $\text{ArCH}_2\text{COO}$ ), 7.0–8.30 (m, 8 H, Ar); IR (KBr pellets) 3080, 2970, 2940, 2910, 2880, 1730, 1620, 1530, 1480, 1450, 1440, 1385, 1370, 1320, 1275, 1210, 1170, 1030, 935, 800, 780, 755, 730, 640  $\text{cm}^{-1}$ ; MS  $m/z$  292 (calcd 292). Anal. Calcd for  $\text{C}_{20}\text{H}_{20}\text{O}_2$ : C, 82.19; H, 6.85; O, 10.99. Found: C, 81.60; H, 6.99; O, 11.09.

**9-[2-(Ethoxycarbonyl)vinylene]-10-ethylanthracene (6).** To a stirred suspension of NaH (1.25 g, 52 mmol) in dried dimethoxyethane (DME, 200 mL) was added dropwise, at room temperature, triethyl phosphonoacetate<sup>16</sup> (12 g, 53 mmol). Stirring was continued for 1 h, and a solution of 9-ethyl-10-formylanthracene<sup>15</sup> (10 g, 43 mmol) in DME (100 mL) was slowly added. The reacting medium turned red. Stirring was continued for 2 h after the addition, and the solution was hydrolyzed with water (200 mL). After the usual workup and crystallization in ethanol, 6 was obtained as red plates (10 g, 76%): mp 110–111 °C;  $^1\text{H NMR}$   $\delta$  1.50 (2 t, 6 H,  $\text{CH}_3\text{CH}_2$ ,  $\text{CH}_3\text{CH}_2\text{OCO}$ ), 3.50 (q, 2 H,  $\text{CH}_3\text{CH}_2\text{Ar}$ ), 7.20–8.40 (m, 8 H, Ar), 6.1–8.6 (AB,  $J = 16$  Hz,  $\text{HC}=\text{CH}$ ); IR (KBr pellets) 3080, 2980, 2940, 2880, 1720, 1635, 1450, 1385, 1370, 1310, 1260, 1230, 1170, 1060, 1030, 990, 930, 880, 850, 760, 720, 645  $\text{cm}^{-1}$ ; MS  $m/z$  304 (calcd 304). Anal. Calcd for  $\text{C}_{21}\text{H}_{20}\text{O}_2$ : C, 82.89; H, 6.58; O, 10.53. Found: C, 82.99; H, 6.66; O, 10.57.

**9-[2-(Ethoxycarbonyl)ethyl]-10-ethylanthracene (7<sub>3</sub>).** Catalytic hydrogenation (atmospheric pressure, room temperature) of ester 6 (2.9 g, 9.5 mmol) over 10% Pd/C (0.5 g) in anhydrous ethanol (100 mL) afforded, after crystallization in aqueous ethanol, 2.3 g (79%) of ester 7<sub>3</sub> as a bright yellow solid: mp 74–75 °C;  $^1\text{H NMR}$   $\delta$  0.90–1.50 (2 t, 6 H,  $\text{CH}_3\text{CH}_2$ ), 2.4–4.3 (m, 8 H,  $\text{CH}_2$ ), 7.1–8.2 (m, 8 H, Ar); IR (KBr pellets) 3080, 2960, 1720, 1480, 1440, 1425, 1290, 1250, 1190, 1040, 740, 640  $\text{cm}^{-1}$ ;  $m/z$  306 (calcd 306). Anal. Calcd for  $\text{C}_{21}\text{H}_{22}\text{O}_2 \cdot \frac{1}{2}\text{H}_2\text{O}$ : C, 80.00, H, 7.30; O, 12.69. Found: C, 80.35; H, 7.21; O, 12.17.

**(9-Ethyl-10-anthryl)acetic Acid (8<sub>2</sub>).** A mixture of 2.0 g (6.8 mmol) of ester 7<sub>2</sub>, 2.0 g (50 mmol) of NaOH, and 100 mL of ethanol was stirred at reflux for 2 h under  $\text{N}_2$  atmosphere. Most of the alcohol was removed under reduced pressure and the brown residue dissolved in the minimum of water. The aqueous solution was cooled and acidified with concentrated HCl. The yellow precipitate was crystallized in benzene, which gave pure 8<sub>2</sub> as pale yellow needles (1.5 g, 83%): mp 258 °C; IR (KBr pellets) 3700–3100, 2950, 1685, 1615, 1440, 1420, 1320, 1270, 1220, 795, 770, 750, 630  $\text{cm}^{-1}$ ; MS  $m/z$  264 (calcd 264). Anal. Calcd for  $\text{C}_{18}\text{H}_{16}\text{O}_2$ : C, 81.82; H, 6.06; O, 12.12. Found: C, 81.06; H, 6.04; O, 12.20.

**$\beta$ -(9-Ethyl-10-anthryl)propionic Acid (8<sub>3</sub>).** Prepared as 8<sub>2</sub> from the ester compound 7<sub>3</sub> (1 g, 3.3 mmol) as a yellow amorphous solid (0.85 g, 93%): mp 146 °C;  $^1\text{H NMR}$   $\delta$  1.40 (t, 3 H,  $\text{CH}_3$ ), 2.4–4.0 (m, 6 H,  $\text{CH}_2$ ), 7.2–8.4 (m, 8 H, Ar), 11.4 (s, 1 H,  $\text{COOH}$ ); IR (KBr pellets) 3600–3100, 2960, 2920, 1700, 1630, 1480, 1450, 1380, 1300, 1260, 1210, 1160, 1100, 800, 750  $\text{cm}^{-1}$ ; MS  $m/z$  278 (calcd 278). Anal. Calcd for  $\text{C}_{19}\text{H}_{18}\text{O}_2 \cdot \text{H}_2\text{O}$ : C, 77.02; H, 6.76. Found: C, 77.81; H, 6.71.

**9-(2,13-Dioxo-6,9,17,20-tetraoxa-3,12-diaza[8<sup>3,12</sup>]docosyl)-10-ethylanthracene (10<sub>2</sub>).** A benzene (50 mL) solution of 1.50 g (6 mmol) of acid chloride 9<sub>2</sub> prepared from acid 6<sub>2</sub> (1.5 g, 5.7 mmol), oxalyl chloride (3.0 g, 24 mmol), and benzene (50 mL) was added dropwise to a solution of the *N*-acetyl-[18]- $\text{N}_2\text{O}_4$  macrocycle<sup>17</sup> (1.5 g, 6 mmol) and triethylamine (1.0 g, 10 mmol) in benzene (100 mL). Then 20 mL of sodium hy-

dride (10%) was added and the mixture was stirred for 15 min. After decantation, the benzene solution was extracted successively with (i) 30 mL of sodium hydroxide (10%), (ii)  $3 \times 20$  mL of hydrochloric acid (10%), and (iii) distilled water up to neutral pH. The organic phase was dried ( $\text{MgSO}_4$ ) and evaporated to give an orange waxy product (2.3 g, 84%):  $^1\text{H NMR}$   $\delta$  1.2 (t, 3 H,  $\text{CH}_3\text{CH}_2\text{Ar}$ ), 1.80 (s, 3 H,  $\text{CH}_3\text{CON}$ ), 3.35 (m, 26 H,  $\text{CH}_2$ ), 4.40 (s, 2 H,  $\text{ArCH}_2\text{CON}$ ), 7.10–8.20 (m, 8 H, Ar); IR (NaCl, film) 3080, 2980, 2940, 2860, 1640, 1450, 1415, 1360, 1350, 1220, 1120, 1030, 910, 780, 760, 730  $\text{cm}^{-1}$ .

**9-(3,14-Dioxo-7,10,18,21-tetraoxa-4,13-diaza[8<sup>4,13</sup>]tricosanyl)-10-ethylanthracene (10<sub>3</sub>).** By the same procedure as above, using 2.0 g (7 mmol) *N*-acetyl-[18]- $\text{N}_2\text{O}_4$  macrocycle, 1.5 g (15 mmol) of triethylamine and 2.0 g (7 mmol) of acid chloride 9<sub>3</sub> (prepared as 9<sub>2</sub>), 10<sub>3</sub> was obtained as an orange pasty product (3.1 g, 83%):  $^1\text{H NMR}$   $\delta$  1.30 (t, 3 H,  $\text{CH}_3\text{CH}_2\text{Ar}$ ), 1.90 (s, 3 H,  $\text{CH}_3\text{CON}$ ), 2.40–4.10 (m, 30 H,  $\text{CH}_2$ ), 7.10–8.40 (m, 8 H, Ar); IR (NaCl, film) 3060, 3020, 2980, 2920, 2860, 1635, 1460, 1440, 1410, 1280, 1200, 1110, 1030, 750, 675  $\text{cm}^{-1}$ .

**Model Compounds M<sub>n</sub>.** They were obtained after reduction of the diamides 10<sub>n</sub> with diborane in THF according to the procedure described for compounds A<sub>nm</sub>.

**9-(6,9,17,20-Tetraoxa-3,12-diaza[8<sup>3,12</sup>]docosyl)-10-ethylanthracene (M<sub>2</sub>).** From 2.3 g (4.2 mmol) of diamide 10<sub>2</sub> and 10 mL of diborane solution (1 M in THF) was obtained pure M<sub>2</sub> after chromatography on neutral alumina (eluent benzene) as an orange oily product (2.0 g, 92%):  $^1\text{H NMR}$   $\delta$  1.10 (t, 3 H,  $\text{CH}_3\text{CH}_2\text{N}$ ), 1.40 (t, 3 H,  $\text{CH}_3\text{CH}_2\text{Ar}$ ), 2.50–3.00 (m, 12 H,  $\text{NCH}_2$ ), 3.50–3.70 (m, 20 H,  $\text{ArCH}_2$ ,  $\text{OCH}_2$ ), 7.50–8.50 (m, 8 H, Ar); IR (NaCl, film) 3080, 2940, 2840, 1610, 1500, 1450, 1370, 1300, 1260, 1130, 1060, 930, 750  $\text{cm}^{-1}$ ; MS  $m/z$  522 (calcd 522). Anal. Calcd for  $\text{C}_{32}\text{H}_{46}\text{N}_2\text{O}_4 \cdot \text{H}_2\text{O}$ : C, 71.11; H, 8.89; N, 5.18. Found: C, 71.80; H, 8.78; N, 4.92.

**9-(7,10,18,21-Tetraoxa-4,13-diaza[8<sup>4,13</sup>]tricosanyl)-10-ethylanthracene (M<sub>3</sub>).** From 3.1 g (5.5 mmol) of diamide 10<sub>3</sub> and 15 mL of diborane solution (1 M in THF) was obtained pure M<sub>3</sub> after chromatography on neutral alumina (eluent benzene) as an orange oily product (2.5 g, 88%):  $^1\text{H NMR}$   $\delta$  0.90 (t, 3 H,  $\text{CH}_3\text{CH}_2\text{N}$ ), 1.40 (t, 3 H,  $\text{CH}_3\text{CH}_2\text{Ar}$ ), 1.80 (m, 2 H,  $\text{ArCH}_2\text{CH}_2\text{CH}_2\text{N}$ ), 2.30–2.90 (m, 12 H,  $\text{NCH}_2$ ), 3.50 (m, 20 H,  $\text{ArCH}_2$ ,  $\text{OCH}_2$ ), 7.20–8.50 (m, 8 H, Ar); IR (NaCl, film) 3080, 2950, 2840, 1620, 1450, 1350, 1260, 1130, 1060, 930, 750, 730, 700, 650  $\text{cm}^{-1}$ ; MS  $m/z$  536 (calcd 536). Anal. Calcd for  $\text{C}_{33}\text{H}_{48}\text{N}_2\text{O}_4$ : C, 73.88; H, 8.96; N, 5.22. Found: C, 73.08; H, 8.98; N, 4.82.

***N,N'*-Diacetyl-[18]- $\text{N}_2\text{O}_4$  Macrocycle.** To a stirred solution of [18]- $\text{N}_2\text{O}_4$  macrocycle (5 g, 19 mmol) and triethylamine (4 g, 41 mmol) in dried benzene (150 mL) was added dropwise acetyl chloride (3.2 g, 41 mmol) in benzene (30 mL). Following the workup used for 8<sub>m</sub>, the expected diamide was obtained as a white solid (6 g, 90%): mp 98 °C;  $^1\text{H NMR}$   $\delta$  2.25 (s, 6 H,  $\text{CH}_3\text{CO}$ ), 3.75 (m, 24 H, " $\text{N}_2\text{O}_4$ " ring); IR (KBr pellets) 3000–2850, 1630, 1480, 1450, 1420, 1350, 1100, 1030, 900  $\text{cm}^{-1}$ ; MS  $m/z$  346 (calcd 346). Anal. Calcd for  $\text{C}_{16}\text{H}_{30}\text{N}_2\text{O}_6$ : C, 55.49; H, 8.67; N, 8.09; O, 27.75. Found: C, 55.53; H, 8.78; N, 8.04; O, 27.59.

***N,N'*-Diethyl-[18]- $\text{N}_2\text{O}_4$  Macrocycle.** According to the procedure described for compounds A<sub>nm</sub>, the diethyl derivative was obtained after reduction of the diamide (2.5 g, 7 mmol) in THF (20 mL) with 15 mL of diborane solution (1 M in THF). After chromatography on neutral alumina (eluent benzene) a transparent oil was obtained; after standing, it gave a white solid (2.0 g, 87%): mp 48 °C;  $^1\text{H NMR}$   $\delta$  0.90 (t, 6 H,  $\text{CH}_3$ ), 2.60 (m, 12 H,  $\text{NCH}_2$ ), 3.40 (m, 16 H,  $\text{OCH}_2$ ); IR (NaCl, film) 3000–2700, 1450, 1340, 1120, 1070, 750, 720  $\text{cm}^{-1}$ ; MS  $m/z$  318 (calcd 318). Anal. Calcd for  $\text{C}_{16}\text{H}_{34}\text{N}_2\text{O}_4$ : C, 60.38; H, 10.69; N, 8.81; O, 20.13. Found: C, 60.20; H, 10.80; N, 9.13; O, 19.78.

**Acknowledgment.** La Région Aquitaine is thanked for partial support of the Centre d'Etudes de la Structure et d'Analyse des Molécules Organiques equipment. The CNRS and the University of Bordeaux I are gratefully acknowledged for financial assistance. We are indebted to Dr. H. Schneider (MPI für Biophysikalische Chemie, Göttingen, Germany) for helpful information concerning the coronand[2.2]. Acknowledgment is also made to the donors of the Petroleum Research Fund, administered by the American Chemical Society.